

PhotoD: LSST photometric distances out to 100 kpc.

GREG J. SCHWARZ ¹, AUGUST MUENCH,¹

(AAS JOURNALS DATA EDITORS)

BUTLER BURTON,^{2,3} AMY HENDRICKSON,^{4,*} JULIE STEFFEN,^{5,1} MAGARET DONNELLY,⁶

¹*American Astronomical Society
1667 K Street NW, Suite 800
Washington, DC 20006, USA*

²*Leiden University*

³*AAS Journals Associate Editor-in-Chief*

⁴*TeXnology Inc.*

⁵*AAS Director of Publishing*

⁶*IOP Publishing, Washington, DC 20005*

ABSTRACT

This example manuscript is intended to serve as a tutorial and template for authors to use when writing their own AAS Journal articles. The manuscript includes a history of AASTeX and documents the new features in the previous versions as well as the bug fixes in version 6.31. This manuscript includes many figure and table examples to illustrate these new features. Information on features not explicitly mentioned in the article can be viewed in the manuscript comments or more extensive online documentation. Authors are welcome to replace the text, tables, figures, and bibliography with their own and submit the resulting manuscript to the AAS Journals peer review system. The first lesson in the tutorial is to remind authors that the AAS Journals, the *Astrophysical Journal* (ApJ), the *Astrophysical Journal Letters* (ApJL), the *Astronomical Journal* (AJ), and the *Planetary Science Journal* (PSJ) all have a 250 word limit for the abstract^{a)}. If you exceed this length the Editorial office will ask you to shorten it. This abstract has 182 words.

Keywords: Distance measure (395) — Interstellar extinction (841) — Photometry (1234) — Stellar distance (1595) — Two-color diagrams (1724)

1. INTRODUCTION

Thanks to the *Vera C. Rubin* observatory's *Legacy Survey of Space and Time* (LSST), for the first time in history, an astronomical catalog will contain more Milky Way stars than there are living people on Earth – of the order 10-20 billion, depending on model assumptions. In order to map the Milky Way in three dimensions, distances to these stars must be accurately estimated. In this paper we describe a method that will deliver

LSST-based stellar distance estimations complementary to *Gaia*'s state-of-the-art trigonometric parallaxes and reach about 10 times further, to approximately 100 kpc. These results will be transformative for the studies of the Milky Way in general, and the stellar and the dark matter halo in particular as never before was there a survey that simultaneously observed roughly two thirds of the sky, to the co-added depth of $r \approx 26$ mag.

A bit about the importance of the distance estimation in the MW, dust implications (for extragalactic science too).

There are a variety of astronomical methods to estimate distances to stars, ranging from direct geometric (trigonometric) methods for nearby stars to indirect methods based on astrophysics for more distant stars.

Corresponding author: August Muench
greg.schwarz@aas.org, gus.muench@aas.org

^{a)} Abstracts for Research Notes of the American Astronomical Society (RNAAS) are limited to 150 words

* AASTeX v6+ programmer

51 Mention Bailer-Jones et al. (2021), Gordon et al.
 52 (2016), Green et al. (2014, 2015, 2019), Jurić et al.
 53 (2008) and Lallement et al. (2014), Queiroz et al. (2018).
 54 Layout of the paper is...

55 2. METHOD

56 The photometric distance estimation method (here-
 57 after **photoD**) is conceptually quite simple and relies on
 58 the strong correlations between the stellar colors and
 59 spectral energy distributions (SED) for dominant stel-
 60 lar populations. The stellar spectral energy distribu-
 61 tions, and consequently colors, are determined by the
 62 effective temperature (T_{eff}), the surface gravity (g), and
 63 the metallicity ($[M/H]$), or alternatively, by the absolute
 64 magnitude in band b (M_b), $[M/H]$ and age.

65 The distributions that describe these correlations are
 66 obtained either from models or from observations. For
 67 example, the distribution of stellar SEDs in the color-
 68 color diagram in Figure 1 provides key insights in stel-
 69 lar evolution and classification of different stellar popu-
 70 lations such as main-sequence stars, giant stars, white
 71 dwarf stars, a majority of unresolved binary stars and
 72 even extragalactic objects. Analogous distributions
 73 are responsible for the abundant structure seen in the
 74 Hertzsprung-Russell diagram (HRD).

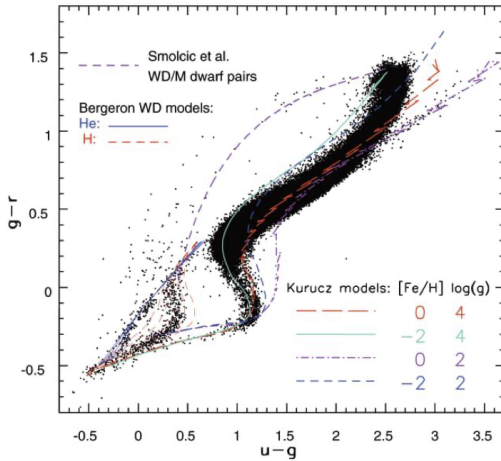


FIG. 23.—The $g-r$ vs. $u-g$ color-color diagrams for all nonvariable point sources constructed with the improved averaged photometry (dots). Various stellar models (Kurucz 1979; Bergeron et al. 1995; Smolčić et al. 2004) are shown by lines, as indicated in the figure.

Figure 1. Color-color diagram. Add a version with overlaid evolutionary tracks in order to emphasize the required precision of the photometry required to disentangle the dwarfs and giants and different metallicities. Are ev. tracks with different metallicities overlapping? Can there be a situation where there is confusion between giants and dwarfs with different metallicities?

75 Metallicity is an important factor in these correla-
 76 tions, as it has a strong effect on the luminosity of the

77 stars. This is reflected in the width of the main stel-
 78 lar loci of the color-magnitude diagrams (CMD) of the
 79 stellar populations observed at the same distance and
 80 the two-color diagrams (quantify), as seen in Figure 2.
 81 The best photometric estimators of metallicity are col-
 82 ors whose shorter-wavelength component includes the
 83 metal absorption bands at near-UV wavelengths, short
 84 of Balmer break ($300 \lesssim \lambda \text{ [nm]} \lesssim 400$). Therefore,
 85 the LSST has a comparative advantage over the sur-
 86 veys lacking u -band measurements, and could provide
 87 accurate distances within the range of 5-10%. A plot
 88 of model spectra, fixed, $\log(g)$ and T_{eff} , several different
 89 metallicities?

THE ASTROPHYSICAL JOURNAL, 783:114 (16pp), 2014 March 10

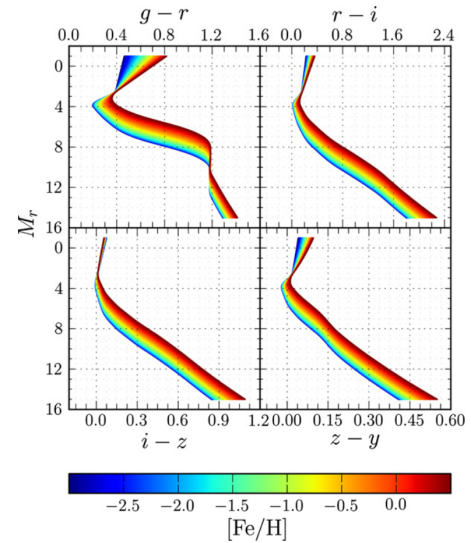


Figure 1. Model stellar colors as a function of absolute r magnitude and metallicity in Pan-STARRS 1 passbands. The stellar templates are based on PS1 color-color relations, and color is related to absolute magnitude and metallicity by SDSS observations of globular clusters (Ivezić et al. 2008a). Our empirical templates therefore assume an old stellar population. While the main sequence below the turnoff is nearly invariant with age, the giant branch and the location of the turnoff do, in reality, vary considerably with age. For this reason, we expect our inferences for main-sequence stars to be more accurate than those for giants. The narrowness of the kink at $M_r \simeq 2.4$ is an artifact of our models (see Section 4.1).

Figure 2. Yadayada.

90 Extinction is another major source of systematic er-
 91 rors in the process of luminosity and distance determi-
 92 nation. The fact that the extinction vector is nearly
 93 parallel to the main stellar locus in the two-color dia-
 94 grams gives rise to degeneracies that complicate the de-
 95 termination of the stellar type. An example is displayed
 96 in Fig. 3, where in the left panel any of the different
 97 star types designated as 1, 2 and 3 can have the same
 98 observed colors as the star marked as "Obs". This de-
 99 generacy is a result of the combination of colors chosen
 100 for the two-color diagram and depends on the position

on the stellar locus and the adopted extinction curve parametrized by a single parameter R_V

$$R_V = \frac{A_V}{E(B-V)}, \quad (1)$$

where A_V stands for extinction in V -band and $E(B-V)$ is the color excess. This relationship can be extended to an arbitrary photometric bandpass λ :

$$A_\lambda = C_\lambda(R_V)A_r, \quad (2)$$

with A_r designating extinction in r -band and $C_\lambda(R_V)$ describing the shape of the extinction curve. The degeneracy from the left panel in Fig. 3 can be broken if several different colors are used, particularly those towards the infrared, where the stellar locus is not kinked and the extinction vector is not parallel to it (as shown in the right panel of the Figure 3), where $r-i$ and $i-z$ colors are used, and assuming a fixed extinction law a unique solution for the extinction is possible.

Explain the choice of R_V .

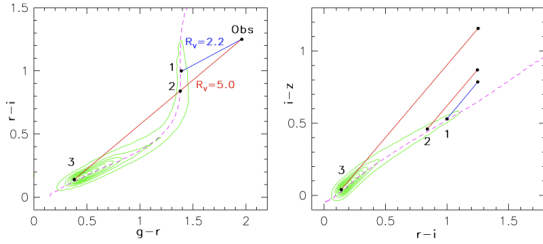


Figure 3. Extinction & degeneracies.

Another important degeneracy arises from the fact that even for a fixed T_{eff} and $[M/H]$, the $\log(g)$ and thus the luminosity are not uniquely determined by the colors: a degeneracy may exist between the giant branch and the main sequence as the colors constructed from $ugrizy$ bands are not sensitive to $\log(g)$ (As evident from Ži's gr-ri plot.). We treat this issue by adopting a prior based on bins in apparent magnitude.

We adopt a Bayesian framework in which we simultaneously fit for M_b , $[M/H]$ and A_r , assuming a fixed R_V value of 3.1¹. The posterior for each individual star with LSST photometry is then given as:

$$\frac{P(M_b, [M/H], A_r | \vec{c})}{P(\vec{c} | M_b, [M/H], A_r) P(M_b, [M/H], A_r)} \quad (3)$$

with \vec{c} standing for the vector of input colors ($u-g$, $g-r$ and so on). The log-likelihood is given by:

¹ In principle R_V could be also fitted for.

$$\ln \mathcal{L} = \frac{-1}{\sqrt{2\pi}} \sum_{i=1}^N \left(\frac{c_i^{\text{obs}} - c_i^{\text{mod}}}{\sigma_i} \right)^2 \quad (4)$$

where c_i^{obs} are the observed colors and c_i^{mod} model colors. The values of model colors and the priors are extracted from TRILEGAL (Dal Tio et al. (2022)). In order to extract the priors (i.e. prior maps), we divide TRILEGAL data in healpix bins, and further subdivide them in one-magnitude wide bins in apparent magnitude. The latter subdivision is helpful in breaking the degeneracies between the giant and dwarf stars, as intrinsically luminous stars become strongly disfavored at faint magnitudes².

Add plots describing the method, and go through one example like in Željko's slides.

Our method is basically brute-force fitting with some intelligent tricks leveraged to obtain faster execution that will be required for 10B LSST stars. We use Schlegel et al. (1998) (SFD98) maps in order to limit the range of the extinction. This is usually a valid assumption because the SFD98 maps provide *total* extinction along a line of sight. Our fitting procedure is also executed on an adaptive grid, a coarse search over the parameter space is performed first in order to establish the layout of the manifold. However, care is taken that any possible local minima are not missed by appropriately adjusting the step size how?. The located maxima are then explored with a smaller step size (adjusted how?). In addition to the approach described here, we also tested Markov Chain Monte Carlo and neural network approaches that will be described in forthcoming/published papers.

Advantages & disadvantages of the model-based and empirical approaches, how model based approaches can be improved by adding empirical information for specific cases.

Gordon et al. (2016) na BEAST webu imaju zgodne diagrame; možda bi i mi mogli nešto tog tipa napraviti, bar za draft, primjer

² In other words, an apparently faint giant star would imply a very large distance. For example a moderately bright giant star with $M_r=0$ mag and $r=22$ mag would imply a distance modulus of 22 mag, or distance of approximately 251 kpc.

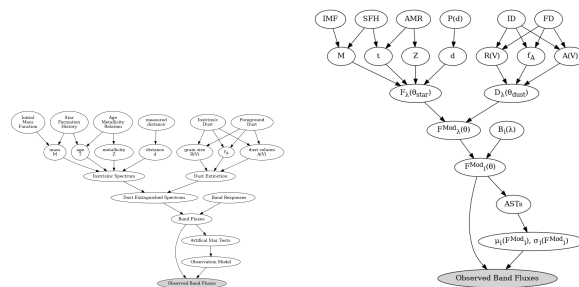


Figure 4. BEAST.

170

171

172

173 Bailer-Jones, C. A. L., Rybizki, J., Foesneau, M.,
174 Demleitner, M., & Andrae, R. 2021, *AJ*, 161, 147,
175 doi: [10.3847/1538-3881/abd806](https://doi.org/10.3847/1538-3881/abd806)
176 Dal Tio, P., Pastorelli, G., Mazzi, A., et al. 2022, *The*
177 *Astrophysical Journal Supplement Series*, 262, 22,
178 doi: [10.3847/1538-4365/ac7be6](https://doi.org/10.3847/1538-4365/ac7be6)
179 Gordon, K. D., Foesneau, M., Arab, H., et al. 2016, *The*
180 *Astrophysical Journal*, 826, 104,
181 doi: [10.3847/0004-637X/826/2/104](https://doi.org/10.3847/0004-637X/826/2/104)
182 Green, G. M., Schlafly, E., Zucker, C., Speagle, J. S., &
183 Finkbeiner, D. 2019, *The Astrophysical Journal*, 887, 93,
184 doi: [10.3847/1538-4357/ab5362](https://doi.org/10.3847/1538-4357/ab5362)
185 Green, G. M., Schlafly, E. F., Finkbeiner, D. P., et al. 2014,
186 *ApJ*, 783, 114, doi: [10.1088/0004-637X/783/2/114](https://doi.org/10.1088/0004-637X/783/2/114)

187 —. 2015, *ApJ*, 810, 25, doi: [10.1088/0004-637X/810/1/25](https://doi.org/10.1088/0004-637X/810/1/25)

188 Jurić, M., Ivezić, Ž., Brooks, A., et al. 2008, *The*

189 *Astrophysical Journal*, 673, 864, doi: [10.1086/523619](https://doi.org/10.1086/523619)

190 Lallement, R., Vergely, J.-L., Valette, B., et al. 2014, *A&A*,

191 561, A91, doi: [10.1051/0004-6361/201322032](https://doi.org/10.1051/0004-6361/201322032)

192 Queiroz, A. B. A., Anders, F., Santiago, B. X., et al. 2018,

193 *Monthly Notices of the Royal Astronomical Society*, 476,

194 2556, doi: [10.1093/mnras/sty330](https://doi.org/10.1093/mnras/sty330)

195 Schlegel, D. J., Finkbeiner, D. P., & Davis, M. 1998, *The*

196 *Astrophysical Journal*, 500, 525, doi: [10.1086/305772](https://doi.org/10.1086/305772)